

Spin-orbit coupling induced Mott transition in $\text{Ca}_{2-x}\text{Sr}_x\text{RuO}_4$ ($0 \leq x \leq 0.2$)

Guo-Qiang Liu

Max-Planck-Institut für Festkörperforschung, D-70569 Stuttgart, Germany

(Dated: October 5, 2018)

We propose a new mechanism for the paramagnetic metal-insulator transition in the layered perovskite $\text{Ca}_{2-x}\text{Sr}_x\text{RuO}_4$ ($0 \leq x \leq 0.2$). The LDA+ U approach including spin-orbit coupling is used to calculate the electronic structures. In Ca_2RuO_4 , we show that the spin-orbit effect is strongly enhanced by the Coulomb repulsion, which leads to an insulating phase. When Ca is substituted by Sr, the effective spin-orbit splitting is reduced due to the increasing bandwidth of the degenerate d_{xz} and d_{yz} orbitals. For $x = 0.2$, the compound is found to be metallic. We show that these results are in good agreement with the experimental phase diagram.

PACS numbers: 71.30.+h, 71.15.Mb, 71.27.+a, 71.20.-b

The layered perovskite $\text{Ca}_{2-x}\text{Sr}_x\text{RuO}_4$ (CSRO) has been intensely studied during recent years since this series of compounds exhibits a variety of interesting physical properties as a function of the Sr concentration x .¹⁻⁸ Sr_2RuO_4 is a p-wave superconductor^{1,9} with a K_2NiF_4 -type structure. The substitution of Ca for Sr causes the RuO_6 octahedra to rotate, and start to tilt at $x = 0.5$.⁵ Following with the structure distortion, CSRO undergoes a series of phase transition from a paramagnetic metal ($0.5 < x < 2$) to a magnetic metal ($0.2 < x < 0.5$), and finally to a Mott insulator ($0 < x < 0.2$).⁴ It is unusual that in the Mott insulating regime the metal-insulator transition temperature (T_{MI}) is higher than the Néel temperature (T_N) of the antiferromagnetic (AFM) phase, which shows that a paramagnetic (PM) insulating phase exists between these transition temperatures.^{5,10,11} For pure Ca_2RuO_4 , the PM insulating regime extends from $T_N = 110$ K to $T_{\text{MI}} = 357$ K.^{2,3,10} This property makes $\text{Ca}_{2-x}\text{Sr}_x\text{RuO}_4$ ($0 < x < 0.2$) different from other AFM Mott insulators.

Recently, Qi *et al.*¹² found that the substitution of the lighter Cr for the heavier Ru strongly depresses T_{MI} in $\text{Ca}_2\text{Ru}_{1-y}\text{Cr}_y\text{O}_4$ ($0 < y < 0.13$), which implies a possible influence of the relativistic spin-orbit (SO) coupling on the Mott transition as pointed out by the authors. It is well known that SO coupling plays an important role in 5d transition-metal oxides. For example, Kim *et al.*¹³ found that Sr_2IrO_4 is a $J_{\text{eff}} = 1/2$ Mott insulator, and they showed that the unusual insulating state can be explained by the combined effect of the SO coupling and Coulomb interaction. In the 4d oxides, the importance of SO coupling is under debate. Mizokawa *et al.*,¹⁴ observed strong SO coupling in Ca_2RuO_4 from their photoemission experiment. Based this finding, they argued that the strong SO coupling in Ca_2RuO_4 would cause a complex electronic configuration. Theoretical studies revealed strong SO effects in Sr_2RuO_4 and Sr_2RhO_4 ,^{15,16} which seemingly support the photoemission experiment. However, Fang *et al.*^{17,18} reported an LDA+ U study of Ca_2RuO_4 . They found the AFM state has a rather simple configuration $xy^{\uparrow\downarrow}xz^{\uparrow}yz^{\uparrow}$ without much influence of the SO coupling. These seemingly inconsistent viewpoints raise a question: what role does the SO coupling

play in CSRO?

In this paper we present electronic structure calculations for $\text{Ca}_{2-x}\text{Sr}_x\text{RuO}_4$ using the LDA+ U method including the SO coupling. We show the combination of the SO coupling and Coulomb repulsion opens a band gap in PM Ca_2RuO_4 . The appearance of the Mott insulating phase is strongly dependent on the tilting of the RuO_6 octahedra, which naturally explains the PM Mott transition in the experimental phase diagram. On the other hand, we find SO has much less influence on the AFM order. We show that these phenomena can be explained by a simple formalism.

All the calculations in this work were performed with the full-potential linear augmented plane wave (FLAPW) within the local-density approximation (LDA), as implemented in package WIEN2K.¹⁹ Two experimental structures⁵ were considered in this work. For Ca_2RuO_4 , we used the structure at 180 K, with the space group Pbcu, lattice constant $a=5.394$, $b=5.600$, and $c=11.765$ Å.⁵ For $\text{Ca}_{1.8}\text{Sr}_{0.2}\text{RuO}_4$, we used the experimental structure at 10 K, but the substitution of Sr for Ca is only taken into account via the structural changes. $\text{Ca}_{1.8}\text{Sr}_{0.2}\text{RuO}_4$ also has the space group Pbcu but with lattice constant $a=5.330$, $b=5.319$, and $c=12.409$ Å.⁵ For the AFM state, we considered the 'A-centered' mode.³ The LDA+ U calculations were performed with $U = 3.0$ eV, which is similar to the value used by Fang *et al.*^{17,18} We will show that this U value can reproduce the measured band gap in Ca_2RuO_4 .

In Fig. 1, we present our theoretical band structures for paramagnetic Ca_2RuO_4 using different approximations. The LDA band structure is well known^{20,21}: the bands crossing the Fermi level are from Ru t_{2g} orbitals, containing four d electrons. Our LDA band structure shown in Fig. 1a is consistent with the previous study.²⁰ The inclusion of the SO coupling (Fig. 1b) only shows some slight changes on the band structure. This is not surprising since the SO coupling constant ζ in Ca_2RuO_4 is presumably similar to the one in Sr_2RuO_4 , where it is only about 93 meV.¹⁵ The inclusion of Coulomb interaction (Fig. 1c) also shows little influence on the band structure since U does not break the orbital symmetry in the paramagnetic state. Surprisingly, the combined inter-

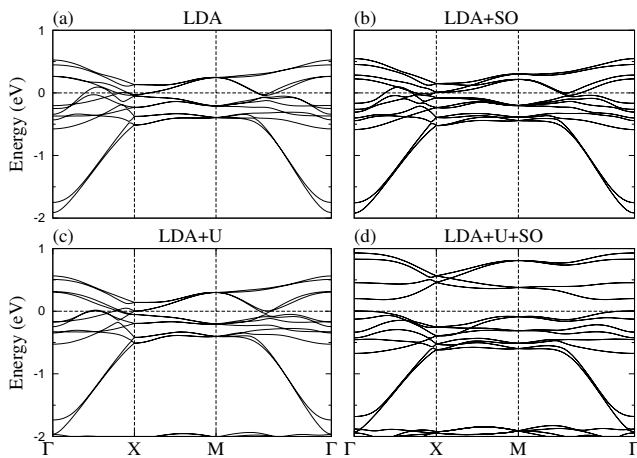


FIG. 1: Theoretical band structures for paramagnetic Ca_2RuO_4 using different approximations, (a) LDA, (b) LDA+SO, (c) LDA+U, and (d) LDA+U+SO. The LDA+U and LDA+U+SO band structures are calculated with $U=3.0$ eV.

action of the SO coupling and Coulomb repulsion gives a very different band structure compared to the LDA, LDA+SO or LDA+U results. The LDA+U+SO band structure shows an insulating phase with a gap about 0.2 eV wide. The band gap obtained from the chosen U is in good agreement with the experimental data.^{2,22}

Similar combined effect of the SO coupling and U has been found in Sr_2RhO_4 ,¹⁶ where it was termed *Coulomb-enhanced spin-orbit splitting*. Sr_2RhO_4 has a similar crystal structure to $\text{Ca}_{2-x}\text{Sr}_x\text{RuO}_4$, and it can be regarded as a two-band (xz and yz) system since the xy band is below the Fermi level due to the RhO_6 rotation.^{23,24} The simpler problem of Sr_2RhO_4 can help us to understand the LDA+U+SO band structure of Ca_2RuO_4 . In Sr_2RhO_4 , the SO coupling splits the degenerate xz and yz bands to the higher $\chi_{\pm 3/2}$ bands, and lower $\chi_{\pm 1/2}$ bands, where

$$\begin{aligned} \chi_{3/2} &= (xz + iy z) \uparrow, & \chi_{-3/2} &= (xz - iy z) \downarrow \\ \chi_{1/2} &= (xz + iy z) \downarrow, & \chi_{-1/2} &= (xz - iy z) \uparrow. \end{aligned}$$

This splitting happens around the Fermi level, and therefore the occupancies of the $\chi_{\pm 3/2}$ and $\chi_{\pm 1/2}$ states are changed: $(n_{1/2} + n_{-1/2}) - (n_{3/2} + n_{-3/2}) = p > 0$, where $n_{1/2} = n_{-1/2}$ and $n_{3/2} = n_{-3/2}$. When the Coulomb interaction is taken into account, the SO splitting is enhanced due to the different occupancies of the $\chi_{\pm 3/2}$ and $\chi_{\pm 1/2}$ states. The interplay the SO coupling and Coulomb interaction can be represented by an effective SO constant¹⁶

$$\zeta_{eff} = \zeta + \frac{1}{2}(U - J)p, \quad (1)$$

where J is the Hund's coupling and p is determined self-consistently.

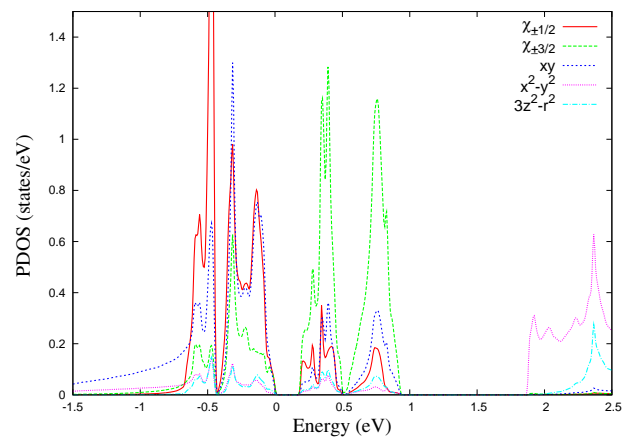


FIG. 2: Ru- d PDOS for paramagnetic Ca_2RuO_4 calculated by LDA+U+SO.

The problem of Ca_2RuO_4 is more complicated than Sr_2RhO_4 since the xy orbital is also involved. Fig. 2 presents the partial density of states (PDOS) for the Ru- d orbitals calculated by LDA+U+SO. Here we present the PDOS for the $\chi_{\pm 3/2}$ and $\chi_{\pm 1/2}$ orbitals instead of xz and yz . The PDOS shows that the unoccupied t_{2g} bands (0.2-0.9 eV) are dominated by the $\chi_{\pm 3/2}$ states while the $\chi_{\pm 1/2}$ states are nearly fully occupied. The well separated $\chi_{\pm 3/2}$ and $\chi_{\pm 1/2}$ states indicate a large effective spin-orbit splitting in Ca_2RuO_4 . Therefore, A simple explanation for the PM Mott transition is that the Coulomb-enhanced spin-orbit splitting opens a gap between the $\chi_{\pm 3/2}$ and $\chi_{\pm 1/2}$ bands, leading to an insulating phase with two holes residing on the $\chi_{\pm 3/2}$ orbitals. In this explanation, the xy state is assumed to be fully occupied. However, in the experimental structure, the xy , xz and yz orbitals hybridize with each other due to the structural distortion. As may be seen, the weight of the xy state in the unoccupied t_{2g} bands is not small as shown in Fig. 2. The relative hole population shown in Fig. 2 is $xy:\chi_{\pm 1/2}:\chi_{\pm 3/2}=19:13:68$, while this ratio is $21:39.5:39.5$ within LDA approximation. This shows that the inclusion of SO and U hardly changes the occupancy of the xy orbital. We may conclude that the band gap is mainly due to the splitting of $\chi_{\pm 3/2}$ and $\chi_{\pm 1/2}$ orbitals although the xy orbital is also involved in the Mott transition.

Experimental research has found that the Mott transition in CSRO is accompanied by an structural phase transition from the high temperature $L\text{-}Pbca$ phase to the low temperature $S\text{-}Pbca$ phase,^{5,11} where L (S) indicates a long (short) c -axis. The phase transition temperature T_S is a function of Sr concentration x , which decreases from 357 K at $x = 0$ to 0 K at $x \sim 0.2$ ^{5,11}. For $x \geq 0.2$, CSRO is metallic and only has the $L\text{-}Pbca$ phase. As indicated by Friedt *et al.*,⁵ the structural transition from the $L\text{-}Pbca$ to $S\text{-}Pbca$ phase is characterized by an increase in the tilting angle of RuO_6 octahedra. We will show that the tilting angle of RuO_6 plays an important role in the Mott transition. To illuminate the

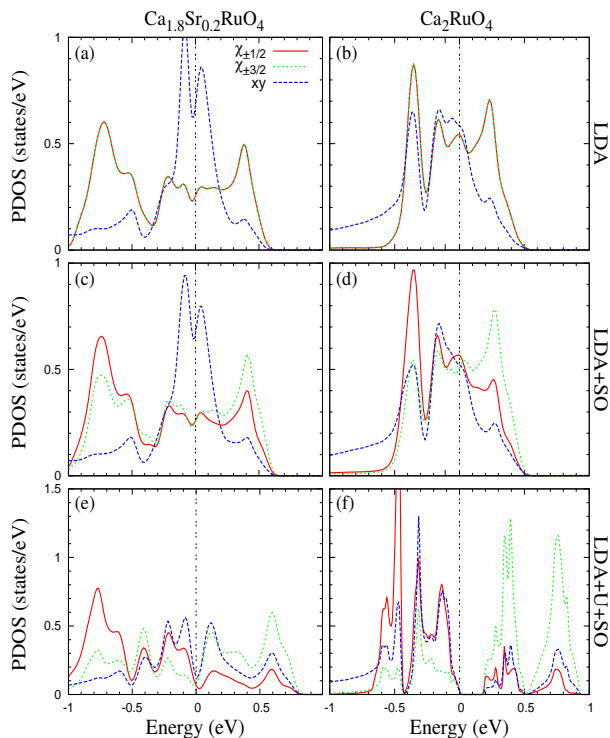


FIG. 3: Ru- t_{2g} PDOS for paramagnetic state using different approximations. The left panels are for $\text{Ca}_{1.8}\text{Sr}_{0.2}\text{RuO}_4$, and right panels for Ca_2RuO_4 .

relation between the Mott transition and the structural phase transition, we apply the LDA+ U +SO calculation to $\text{Ca}_{1.8}\text{Sr}_{0.2}\text{RuO}_4$.

Fig. 3 presents our calculated PDOS for $x = 0.2$ (L - $Pbca$) and $x = 0$ (S - $Pbca$). Fig. 3a and 3b show the LDA PDOS for $x = 0.2$ and $x = 0$. The xz/yz bandwidth is about 1.6 eV in $\text{Ca}_{1.8}\text{Sr}_{0.2}\text{RuO}_4$, and it is reduced to 1.1 eV in Ca_2RuO_4 . The narrower xz/yz band in Ca_2RuO_4 is due to its larger tilting angle. The tilting angle is about 12° in Ca_2RuO_4 , and it is 6° in $\text{Ca}_{1.8}\text{Sr}_{0.2}\text{RuO}_4$.⁵ The tilting of the in-plane Ru-O can significantly reduce the interaction between Ru- $d_{xz/yz}$ and O- p_z . Consequently, the xz/yz bandwidth decreases from $x = 0.2$ to $x = 0$, while the xy bandwidth is less influenced. With the narrower xz/yz band, Ca_2RuO_4 shows much higher xz/yz PDOS around the Fermi level than $\text{Ca}_{1.8}\text{Sr}_{0.2}\text{RuO}_4$. Fig. 3c and 3d show the LDA+SO PDOS for $x = 0.2$ and $x = 0$. As may be seen, the occupancy difference between the $\chi_{\pm 3/2}$ and $\chi_{\pm 1/2}$ states is larger in Ca_2RuO_4 than in $\text{Ca}_{1.8}\text{Sr}_{0.2}\text{RuO}_4$. This is understandable if we consider the higher PDOS in Ca_2RuO_4 . Eq. (1) shows the effective SO splitting is proportional to the occupancy difference p . Then the larger occupancy difference p in Ca_2RuO_4 will cause larger SO splitting when Coulomb interaction is taken into account. This is confirmed by the LDA+ U +SO PDOS shown in Fig. 3e and 3f. Using Eq. (1), we get $\zeta_{eff} = 0.9$ eV for Ca_2RuO_4 , and 0.6 eV for $\text{Ca}_{1.8}\text{Sr}_{0.2}\text{RuO}_4$. The larger SO splitting in Ca_2RuO_4

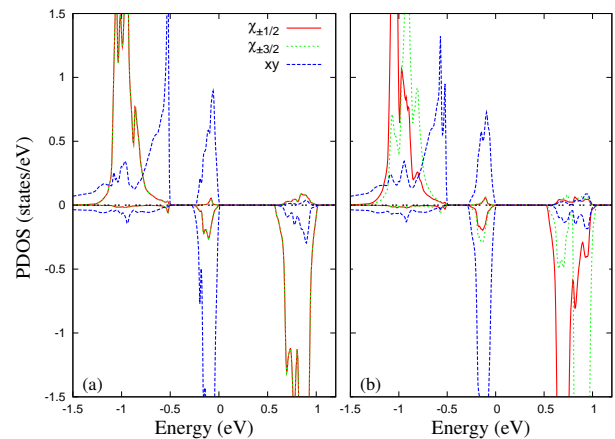


FIG. 4: Ru- t_{2g} PDOS for AFM Ca_2RuO_4 using different approximations, (a) LDA+ U , and (b) LDA+ U +SO.

leads an insulating phase, while $\text{Ca}_{1.8}\text{Sr}_{0.2}\text{RuO}_4$ remains metallic. Therefore, we have shown that the PM Mott transition in CSRO can be explained by the interplay of SO coupling, Coulomb interaction and structural distortion.

CSRO is a single-layer system, where the t_{2g} bands are split into the singly degenerate xy band and doubly degenerate xz/yz bands. The bare SO coupling mainly influences the degenerate bands since Ru has a moderate SO constant. Therefore, the SO induced Mott transition is strongly orbital dependent. Fig. 3 indicates that the Mott transition in PM CSRO is driven by the narrowing of the xz and yz bands, while the xy orbital plays a less important role. This strong orbital-dependence could also be seen from Eq. (1). The bare SO parameter ζ is constant for each orbital, but the Coulomb enhanced SO parameter ζ_{eff} is a function of orbital occupancies. This suggests that the strong orbital-dependence is an inherent feature of the SO induced Mott transition.

Our calculation has shown that the PM insulating phase of CSRO originates in the strong effective SO splitting. This picture supports the photoemission measurement by Mizokawa *et al.*¹⁴ The suppression of T_{MI} in $\text{Ca}_2\text{Ru}_{1-y}\text{Cr}_y\text{O}_4$ ¹² can also be understood within this picture. Cr has a much smaller atomic SO constant than Ru due to its smaller mass. And therefore the substitution of Cr for Ru will reduce the SO splitting, leading to the observed decrease of T_{MI} .

As mentioned above, Fang *et al.*^{17,18} found that SO coupling has no much influence on the electronic configuration. They however pointed out that the photoemission measurement was done above the Néel temperature, while they applied the LDA+ U method to the low temperature AFM state. To clarify if the SO coupling is less important in AFM state, we apply the LDA+ U and LDA+ U +SO calculation to AFM Ca_2RuO_4 . Our LDA+ U calculation gives a magnetic moment of $m_{\text{Ru}} = 1.25 \mu_B$, which is consistent with Fang *et al.*'s calculation¹⁷; while SO reduces the moment to

1.21 μ_B , showing a weak SO effect. The AFM PDOS for Ca_2RuO_4 are presented in Fig. 4. In contrast to the PM state, Fig. 4 shows that there is no Coulomb-enhanced SO splitting in the AFM state. The relative weak SO splitting in the AFM state can be explained by Eq. (1). The LDA+ U calculation produces an insulating phase for AFM Ca_2RuO_4 as shown in Fig. 4a. Since there is no density of states around the Fermi level, SO coupling can not change the orbital occupancies, which gives $p = 0$. Then we get $\zeta_{eff} = \zeta$, showing no enhanced SO splitting. It is noticeable that our calculations give an AFM ground state for Ca_2RuO_4 , which is consistent with the experimental phase diagram.⁵

Comparing the PM and AFM insulating phases in CSRO, we may find that the two kinds of Mott transition are similar. They both have an interaction to break the orbital symmetry. The interaction is SO coupling in the PM state and spin polarization in the AFM state. The breaking of orbital symmetry lifts the degenerate bands and changes the orbital occupancies. When the Coulomb interaction is taken into account, the orbital splitting, which is SO splitting in the PM state or exchange splitting in the AFM state, is enhanced. If the enhanced splitting is large enough, it will lead to an in-

insulating phase. The PM-AFM transition at T_N can be regarded as the competition of the Coulomb-enhanced SO splitting and the Coulomb-enhanced exchange splitting. In the AFM state, the SO enhancement is quenched by the large exchange splitting, which causes the very different electronic configuration from the PM state.

In summary, we have applied LDA+ U +SO calculations to CSRO. We find the Coulomb enhanced SO splitting produces an insulating phase in PM Ca_2RuO_4 . This finding is consistent with the photoemission experiment, and also explains the recent experiment on $\text{Ca}_2\text{Ru}_{1-y}\text{Cr}_y\text{O}_4$. We show that the SO induced Mott transition in CSRO is driven by the change of the xz/yz bandwidth. For $x = 0.2$, the compound is found to be metallic. On the other hand, we find that SO coupling has much less influence on the AFM state, which is in agreement with the previous LDA+ U study. The above picture shows that SO coupling plays a very subtle role in the correlated systems. The interplay of SO coupling, electron correlation and crystal structure distortion would cause very rich physical phenomena.

The author gratefully acknowledges Ove Jepsen for helpful discussions and useful comments.

-
- ¹ Y. Maeno, H. Hashimoto, K. Yoshida, S. Nishizaki, T. Fujita, J. G. Bednorz, and F. Lichtenberg, *Nature (London)* **372**, 532 (1994).
- ² G. Cao, S. McCall, M. Shepard, J. E. Crow, and R. P. Guertin, *Phys. Rev. B* **56**, R2916 (1997).
- ³ M. Braden, G. Andre, S. Nakatsuji, and Y. Maeno, *Phys. Rev. B* **58**, 847 (1998).
- ⁴ S. Nakatsuji and Y. Maeno, *Phys. Rev. Lett.* **84**, 2666 (2000).
- ⁵ O. Friedt, M. Braden, G. Andre, P. Adelman, S. Nakatsuji, and Y. Maeno, *Phys. Rev. B* **63**, 174432 (2001).
- ⁶ O. Friedt, P. Steffens, M. Braden, Y. Sidis, S. Nakatsuji, and Y. Maeno, *Phys. Rev. Lett.* **93**, 147404 (2004).
- ⁷ M. Kriener, P. Steffens, J. Baier, O. Schumann, T. Zabel, T. Lorenz, O. Friedt, R. Muller, A. Gukasov, P. G. Radaelli, P. Reutler, A. Revcolevschi, S. Nakatsuji, Y. Maeno, and M. Braden, *Phys. Rev. Lett.* **95**, 267403 (2005).
- ⁸ E. Gorelov, M. Karolak, T. O. Wehling, F. Lechermann, A. I. Lichtenstein, and E. Pavarini, *Phys. Rev. Lett.* **104**, 226401 (2010).
- ⁹ A. P. Mackenzie and Y. Maeno, *Rev. Mod. Phys.* **75**, 657 (2003).
- ¹⁰ S. Nakatsuji, S. Ikeda, and Y. Maeno, *J. Phys. Soc. Jpn.* **66**, 1868 (1997).
- ¹¹ C. S. Alexander, G. Cao, V. Dobrosavljevic, S. McCall, J. E. Crow, E. Lochner, and R. P. Guertin, *Phys. Rev. B* **60**, R8422 (1999).
- ¹² T. F. Qi, O. B. Korneta, S. Parkin, L. E. De Long, P. Schlottmann, and G. Cao *Phys. Rev. Lett.* **105**, 177203 (2010).
- ¹³ B. J. Kim, Hosub Jin, S. J. Moon, J.-Y. Kim, B.-G. Park, C. S. Leem, Jaejun Yu, T. W. Noh, C. Kim, S.-J. Oh, J.-H. Park, V. Durairaj, G. Cao, and E. Rotenberg, *Phys. Rev. Lett.* **101**, 076402 (2008).
- ¹⁴ T. Mizokawa, L. H. Tjeng, G. A. Sawatzky, G. Ghiringhelli, O. Tjernberg, N. B. Brookes, H. Fukazawa, S. Nakatsuji, and Y. Maeno, *Phys. Rev. Lett.* **87**, 077202 (2001).
- ¹⁵ M. W. Haverkort, I. S. Elfimov, L. H. Tjeng, G. A. Sawatzky, and A. Damascelli, *Phys. Rev. Lett.* **101**, 026406 (2008).
- ¹⁶ Guo-Qiang Liu, V. N. Antonov, O. Jepsen, and O. K. Andersen, *Phys. Rev. Lett.* **101**, 026408 (2008).
- ¹⁷ Zhong Fang, Naoto Nagaosa, and Kiyoyuki Terakura, *Phys. Rev. B* **69**, 045116 (2004).
- ¹⁸ J. H. Jung, Z. Fang, J. P. He, Y. Kaneko, Y. Okimoto, and Y. Tokura, *Phys. Rev. Lett.* **91**, 056403 (2003).
- ¹⁹ P. Blaha *et al.*, Computer code WIEN2K, TU Wien, Vienna, 2001.
- ²⁰ L. M. Woods, *Phys. Rev. B* **62**, 7833 (2000).
- ²¹ Z. Fang and K. Terakura, *Phys. Rev. B* **64**, R020509 (2001).
- ²² A. V. Puchkov, M. C. Schabel, D. N. Basov, T. Startseva, G. Cao, T. Timusk, and Z.-X. Shen, *Phys. Rev. Lett.* **81**, 2747 (1998).
- ²³ B. J. Kim, Jaejun Yu, H. Koh, I. Nagai, S. I. Ikeda, S.-J. Oh, and C. Kim, *Phys. Rev. Lett.* **97**, 106401 (2006).
- ²⁴ Eunjung Ko, B. J. Kim, C. Kim, and Hyoung Joon Choi, *Phys. Rev. Lett.* **98**, 226401 (2007).